Journal of Theoretical and Applied Information Technology
31st December 2023. Vol.101. No 24

ISSN: 1992-8645 www.jatit.org E-ISSN: 1817-3195

SKIN LESION SEGMENTATION AND CLASSIFICATION USING FCN-ALEXNET FRAMEWORK

V. AUXILIA OSVIN NANCY[1], V.RAJASEKAR[2], MEENAKSHI S ARYA[3]

[1,2] Dept. of Computer science and Engineering, College of Engineering and Technology, SRM Institute of Science and Technology, Vadapalani Campus,Chennai-26, Tamil Nadu,India

[3]Department of Transportation, IOWA State University, IOWA, United States

E-mail: [1]auxilianancy@gmail.com_, [2]brahmaasthra@gmail.com__,[3]raina.arya@gmail.com

ABSTRACT

Malignant melanoma tumors diagnosis relies as essential tasks for segmentation and classification of skin lesion. However, previous deep learning methods still face challenges in effectively handling aspects like boundary identification, artifact presence, and limited dataset availability. The automatic application poses significant difficulties, especially considering the intricate nature of melanoma. Its inconspicuous contrast with surrounding skin makes it a formidable task for clinicians to detect. This research governs the approach that leverages medical image segmentation to aid dermatologists in swift melanoma identification. The AlexNet framework is used in this study to develop a skin lesion segmentation and classification system. It begins with an encoder-decodifier fully convolutional network (FCN) to recognise the complex features of lesions and to learn about their boundaries using the decoder. Using a succession of skip paths, FCN subnetworks are connected to each other. The implementation involves the modification of two CNN architectures into fully convolutional network models. Four distinct FCN architectures, namely modified FCN-AlexNet, FCN-8s, FCN-16s, and FCN-32s, are employed to autonomously dissect skin lesions based on their semantic characteristics. The evaluation on the HAM 10000 dataset, a pivotal aspect of this study, marks the pioneering assessment of their capabilities on this dataset. Through these advancements, this research seeks to enhance the diagnostic accuracy and efficiency of melanoma identification in dermatology.

Keywords: *Skin Lesion, Classification, FCN, Alexnet, Melanoma, Encoder-Decoder, Deep Learning*

1.INTRODUCTION

1.1 Skin Cancer

Skin cancer is a cancer type that occurs in the skin cells. It happens when skin cells mutate, usually as a result of extended exposure to UV radiation from the sun or from artificial sources such as tanning beds. Because of this mutation, the cells grow fast and create cancerous tumours.

The common cancer includes malignant melanoma and also the non-melanoma skin cancers (NMSC's) consisting of basal cell carcinoma (BCC), and squamous cell carcinoma (SCC) as shown in Fig.1 [10]. The description on each type is given below.

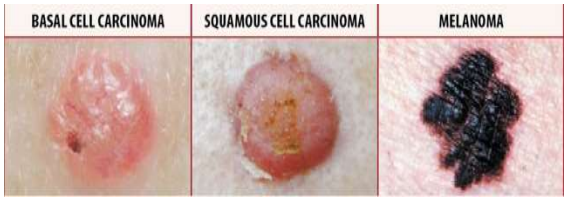

Fig.1 Types of Skin cancer [10]

1.1.1 BCC

This type has been developed in the cells of basal which are found in the skin's innermost layer and typically appears as a raised, pearly bump and doesn't heal. While it grows slowly and seldom spreads to other parts, early discovery and treatment are critical to preventing tissue damage.

1.1.2 SCC

It forms in higher layers but is more prone to spread than BCC. It often appears as a red, scaly patch or a thick, rough, or wart-like growth. SCC can develop from pre-existing conditions like actinic keratosis, which are dry, scaly patches caused by prolonged sun exposure.

1.1.3 Melanoma

Melanoma is the most dangerous form of skin cancer. It develops in melanocytes, the skin cells responsible for producing pigment. Melanoma can appear as a new mole or a change in an existing mole. It's often characterized by irregular borders,

variations in color, and an evolving shape. If not caught early, melanoma can spread to other parts of the body and become life-threatening.

The most fatal kind of cancer in humans, melanoma leaves a colored mark on the skin in the form of a mole. Clinical screening, dermoscopic pictures, histological examination, and biopsy are all used in the first diagnosis of cancer [2].The risk factors for skin cancer includes UV Exposure, Fair Skin, Moles, Family History, and Weakened Immune System. Early detection and prevention play crucial roles in addressing skin cancer. Protecting the skin from excessive sun exposure, using sunscreen, putting on protective clothing, and avoiding tanning beds are essential preventive measures. Regular self-examinations of the skin and professional dermatological screenings can aid in detecting potential skin cancers at an early, more treatable stage.

Skin cancer underscores the importance of public awareness, education, and timely medical intervention. Efforts to promote sun safety, regular check-ups, and technological advancements in detection methods are pivotal in reducing the impact of skin cancer on individuals and society as a whole.

1.2 Traditional Methods for Medical Imaging

Before deep learning concept emerged, we were into the traditional methods for medical imaging analysis. The primary process of traditional methods was feature extraction, statistical analysis, and classical machine learning algorithms.

1.2.1 Image preprocessing

Preprocessing techniques such as noise reduction, image enhancement, and normalization are essential steps before analysis. These methods help improve the quality of images and enhance the visibility of relevant features.

1.2.2 Feature extraction

Handcrafted features are manually designed characteristics extracted from medical images. They can include texture features (e.g., Haralick features), shape features (e.g., area, perimeter), and intensity-based features (e.g., mean, standard deviation).

1.2.3 Edge detection

Edge detection algorithms, like the Canny edge detector, identify abrupt changes in pixel intensity, which can help identify boundaries and important structures in medical images.

1.2.4 Thresholding

Thresholding techniques segment images into binary regions based on pixel intensity values. This is commonly used for segmenting structures of interest from background.

1.2.5 Region of Interest (ROI) Analysis

Identifying and analyzing specific regions within an image can provide insights into certain medical conditions. ROI analysis involves measuring features within these regions.

1.2.6 Histogram analysis

Histograms of pixel intensities provide information about the distribution of image data. Histogram analysis can be used for tissue characterization and distinguishing between different tissue types.

1.2.7 Statistical analysis

Classical statistical techniques can be applied to medical images to quantify differences between populations or assess the significance of certain features.

1.2.8 Segmentation

Traditional segmentation methods aim to separate the image into meaningful regions, such as identifying organs or tumors. Methods like region-growing, watershed segmentation, and active contours are commonly used.

1.2.9 Classification algorithms

Classical machine learning algorithms like decision trees, random forests, support vector machines, and k-nearest neighbors are applied for tasks like disease classification and outcome prediction.

1.2.10 Principal component analysis (pca)

PCA is used to reduce the dimensionality of data while retaining important information. It can help in visualizing data and identifying patterns.

1.2.11 Mathematical modelling

Mathematical models based on differential equations or physical principles can be used for simulating physiological processes or disease progression.

1.3 Deep Learning In Segmentation And Classification Of Medical Image

Deep learning has revolutionized the field of medical image analysis, particularly in the segmentation and classification of medical images. With its capacity to automatically take in characteristics from data, deep learning techniques have shown remarkable performance in accurately identifying and delineating structures in medical images. The two main purposes of deep learning in medical image are segmentation and classification. The segmentation technique applied to the ground

truth to choose the tumor's location. Medical images are classified via classification, and the results of this procedure are used for diagnosis and prediction.

1.3.1 Segmentation

Medical image segmentation involves partitioning an image into meaningful regions to isolate specific structures or objects of interest. Deep learning models, particularly CNN, have excelled in this task due to their ability to capture complex spatial features. Techniques include:

1.3.1.1 U-Net architecture

This architecture is widely used to segment biomedical picture. It includes a path that contracts (encoding) to capture context and a symmetric expanding path (decoding) to achieve precise localization.

1.3.1.2 FCNs (Fully Convolutional Networks)

FCNs are designed for pixel-wise classification, enabling them to produce dense output maps in order to segment images. They take advantage of convolutional layers for feature extraction and up-sampling layers for accurate segmentation.

1.3.1.3 3D Segmentation

For volumetric medical images such as CT scans or MRI, 3D CNNs are employed. These networks consider spatial relationships in three dimensions, enabling more accurate segmentation of structures.

1.3.2 Classification

Medical image classification involves categorizing images into predefined classes, aiding in disease diagnosis and treatment planning. Deep learning models have demonstrated outstanding performance in this area, especially for large datasets. Techniques include:

1.3.2.1 CNN architectures

CNNs excel in extracting hierarchical features from images, making them suitable for medical image classification. Transfer learning using pre-trained models enhances performance when labeled data is limited.

1.3.2.2 Ensemble Learning

Combining the results of various models' predictions can improve classification accuracy. Techniques like bagging and boosting are applied to model deep learning to enhance their robustness.

1.3.2.3 Attention Mechanisms

These mechanisms focus on salient regions in an image, enabling the model to pay more attention to relevant features. This is particularly useful when certain regions carry crucial diagnostic information.

1.3.2.4 Explainable AI

For medical applications, it is crucial to be articulative. Techniques like Grad-CAM provide visual explanations of the features contributing to the model's decision, aiding clinicians in understanding and trusting the predictions.

1.3.3 Applications of Deep Learning in Medical Image Analysis

1.3.3.1 Tumor Detection

Deep learning models can identify tumors in radiology images like MRI and CT scans, aiding in early detection and treatment planning.

1.3.3.2 Retinal Disease Diagnosis

CNNs are used to classify retinal images, helping diagnose conditions like diabetic retinopathy and age-related macular degeneration.

1.3.3.3 Histopathology Analysis

CNNs can identify cancerous cells in histopathology images, aiding in cancer diagnosis and grading.

1.3.3.4 Brain Image Analysis

Deep learning techniques segment brain structures and detect anomalies in neuroimaging, assisting in neurological disorder diagnosis.

1.3.3.5 Skin Lesion Analysis

Models can segment and classify skin lesions, contributing to dermatological diagnoses, including skin cancer detection.

In this article, the skin lesion analysis has been done through the deep learning techniques.

1.4 Deep learning in Skin lesion Analysis

Deep learning has made significant advancements in various fields, including medical image analysis, and skin lesion analysis is no exception. Skin lesion analysis involves the classification, detection, and segmentation of various types of skin lesions, such

as moles, melanomas, and other dermatological conditions. Deep learning techniques, particularly convolution neural networks (CNNs), have shown remarkable success in automating and improving the accuracy of these tasks.

The first step in image classification is to determine whether or not a picture is acceptable and how that acceptance is defined by the class to which it belongs. Human vision is fundamentally different from that of a computer when it comes to identifying images. Pixels are used by the machine to identify the images. Images are sent into a convolution, nonlinear and FCN (completely connected layer) network, which forms the final output after all the layers are processed [12].

1.5 Research Contribution

An extensive experimental set is created using FCN designs. A detailed analysis of the FCN topologies is provided in order to aid in the earliest potential melanoma detection. Comprehensive results are compared to show the effectiveness of FCNs in medical picture segmentation applications, especially for skin lesions.

2 LITERATURE REVIEW

2.1 Review On Skin Cancer Detection Using Machine Learning & Deep Learning Algorithms

In S. Mane.et.al.[9] Support vector machine and Bayesnet classifier for skin cancer diagnosis from the supplied dataset PH2. The performance was examined in two ways by the author. First, the dataset is assumed to have 80 percent and 20 percent training and testing data, and the other 70 percent and 30 percent of the training and testing data is assumed. (80/20) performed better than (70/30) in 92.30% of cases, according to the technique used. The strategy will be tested with a larger dataset in the future.

In M. A. Farooq.et.al.[4], SVM and Neural Classifiers were used to identify and classify lesions by the author. Pre-processing, autonomous segmentation, feature extraction, and classification were all part of this procedure. We will be able to better understand the images if we increase the quantity of dataset photos and the region of interest.

R D, S. et.al.[15], In this article, the author did lesion segmentation and classification using SVM, and the performance was analyzed with accuracy as 85.19%.

In M, V. M.et.al.[8], Image processing and a machine learning system were used to detect skin cancer. The author used image processing techniques such as shade removal, glare reduction, and prediction classification using SVM to prepare the image for the final processing step. The ISIC dataset is compatible with this method.

In Munia, T. T.et.al[14], The author involved the images with linear and nonlinear features of digital images to detect the melanoma. The classification process was done by SVM with an accuracy of 89.07%.In S. Mukherjee.et.al.[13], The author implemented the model using CNN with the cross-platform dataset Dermofit and MEDNODE, and accuracy was obtained of 90.58%. The author worked with the model named CNN –AlexNet using the PH2 dataset in R. Lakhtakia et.al.[7],In this methodology, the author implemented the model using CAD and achieved an accuracy of 97%.

According to the literature study, machine learning and deep learning algorithms have approaches for identifying skin cancer. The performances have been judged on the basis of their accuracy. When it comes to enhancing accuracy, deep learning algorithms are better than machine learning algorithms.

2.2 Review on Skin lesion segmentation and classification

In Sumithra.et.al.[26], color and text features are extracted from region growing method and classification has been done with SVM with KNN and the model evaluated with accuracy 86%.
Lynn.et.al [27] exposed the feature of skin lesion using ABCD rule. The selected optimized features are classified using KNN, SVM, and decision tree classifiers.
In Ünver, H. M. et.al [28], the author has done skin lesion segmentation using the combo of yolo and grab cut algorithm with the accuracy of 90%.
The survey concludes that most of the research articles concentrated on either segmentation or classification and that leads the better accuracy of 90%. The combo of segmentation and classification, the research has done in less number. To increase the performance of the model both in segmentation and classification the model has to be proposed.
This paper proposes the use of AlexNet's FCN-based AlexNet framework for the classification and segmentation of skin lesions.

3 METHODOLOGY USED

Feature extraction and lesion categorization are part of the proposed system's pre-processing step. There are two pieces to it. System Flow A) and System Architecture B). By using a pictorial representation, a flow diagram depicts how the system operates and the steps that are required to complete it. Each phase of the architecture diagram included a description of the methodology used. [9].

3.1 System Flow

Automatic Melanoma cancer detection contains three steps: Analysis of the data prior to its classification. A skin image serves as the system's first input, as depicted in Figure 2. The pre-processing begins by eliminating the hair around the tumor from the input image. The quality of the image produced by this method is excellent. Skin lesion segmentation technique is used to separate the affected area of the skin into separate segments (Encoder and Decoder). Classification (FCN-AlexNet) is used to determine if the image is a benign lesion or a malignant tumor [9].

3.2 System Architecture

This model's construction is depicted in Fig.3. Criteria for the framework include the following:
1. Pre-Processing
2. Skin lesion Segmentation
(i) Encoder-Decoder Segmentation
3. Skin lesion Classification
(i) FCN based AlexNet Framework

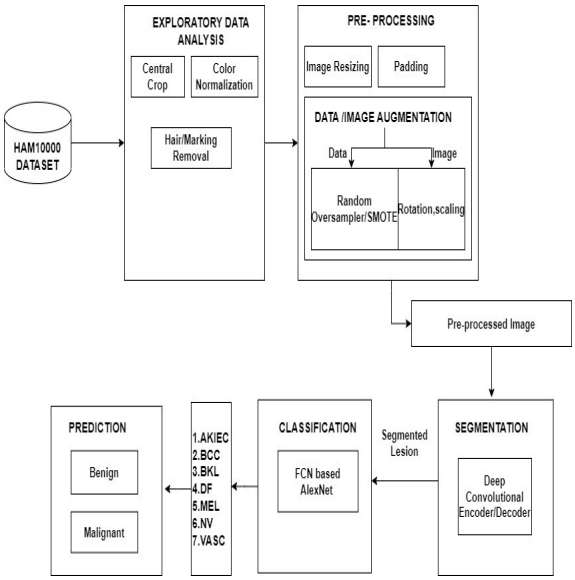

Fig.2 System Flow Diagram

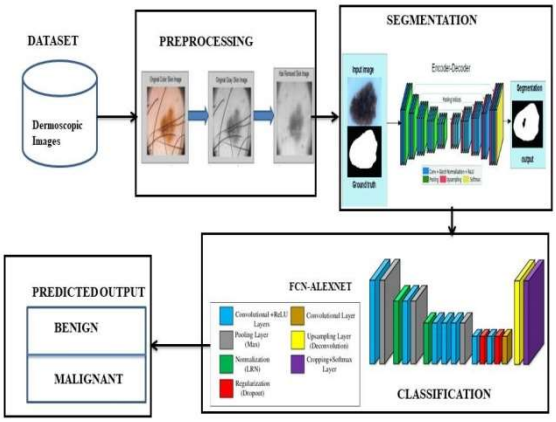

Fig.3 System Architecture

3.2.1 Pre-processing

Pre-processing eliminates the important properties which affect the accuracy of detection such as background noise, skin patches, hair and air bubbles [9].
In this model, skin image is fed as input to the system. The factors which reduce the result of segmentation and classification are the unwanted things like hair and air bubbles which are available in the image.
The following steps are required to make the images with quality and balanced.

3.2.1.1 Central crop

By central cropping the image, extra round black borders and padding are mostly removed and the lesions are enlarged too. By using central crop method the image has been cropped with 85% of centre.

3.2.1.2 Color Normalization

Color normalization has been done by white balancing grey world technique. The Grey World Technique is a color correction method used in image processing to balance the colors in an image. It assumes that in an average image, the colors should appear neutral or "grey".

Let R_avg,G_avg, and B_avg represent the average values of the red, green, and blue color channels in an image, respectively. The Grey World Technique adjusts the color channels so that their averages are equal. This can be expressed mathematically as:

$$R' = \frac{R}{R\_avg} \quad (1)$$

$$G' = \frac{G}{G\_avg} \quad (2)$$

$$B' = \frac{B}{B\_avg} \quad (3)$$

Where R', G', and B' represent the adjusted red, green, and blue channels, respectively. After applying these adjustments, the image should have a balanced color cast, assuming that the original image had an overall color cast that needed correction. This technique is a simple global color correction method.

3.2.1.3 Black hair and markings removal

This process pre-processing was done in two steps [9]:

Step 1: To convert the color image I_{RGB} consisting of three channels (R, G, B) into gray-scale image using the following conversion model.

$$I_g = 0.2989 * R + 0.5870 * G + 0.1140 * B \quad (4)$$

Step 2: Apply the Gaussian filter for removing hair in the image.

$$I_F = gaussian(I_g) \quad (5)$$

Gaussian value can be achieved using the following representation

$$G\sigma = \frac{1}{2\pi\sigma^2} e^{-\frac{(x^2+y^2)}{2\sigma^2}} \quad (6)$$

After completion the results may be expected to be in the form of images as shown in Fig.4

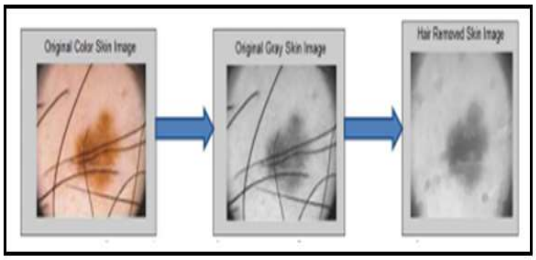

(a)Original Image I_{RGB} (b)Gray Scale Image I_g (c) Hair Removed Image I_F

Fig4: Artifacts Removal

3.2.2 Augmentation

3.2.2.1 Random Resampling

Random resampling techniques involve manipulating the dataset by either oversampling the minority class or under sampling the majority class.

***Random Oversampling*:** Random oversampling involves randomly selecting examples from the minority class and replicating them in the training dataset. By increasing the number of instances in the minority class, random oversampling helps to balance the class distribution and provide more training data for the minority class.

***Random Undersampling*:** Random undersampling, on the other hand, involves randomly selecting examples from the majority class and removing them from the training dataset. This approach reduces the dominance of the majority class, addressing the class imbalance issue by achieving a more balanced class distribution.

Both random oversampling and random undersampling can be used individually or in combination to create a more balanced dataset for training the skin lesion classification model. These techniques aim to improve the model's ability to learn from both the minority and majority classes, leading to better classification performance.

3.2.2.1.1 Algorithm

Input: Imbalanced Training Dataset $(\boldsymbol{T_iD})$
Output: Balanced Training Dataset $(\boldsymbol{B_iD})$

1. **Group**$(\boldsymbol{T_iD})$ by the specification of class
2. $\boldsymbol{M_1}$ => Minor class with less number of instances
3. $\boldsymbol{M_2}$ => Major class with more number of instances
4. For i in rows of $(\boldsymbol{M_1})$
5. For j in rows of $(\boldsymbol{M_2})$
6. $\boldsymbol{Sim_{i,j}}$ = calculate the similarity index between $\boldsymbol{M_2(i)}$ and $\boldsymbol{M_1(j)}$
7. Append to decision samples
8. $\boldsymbol{P}: \prod_{i=1}^{l} \boldsymbol{I}^{|\boldsymbol{F}|} \rightarrow \boldsymbol{I}^{|\boldsymbol{F'}|}$ P -> l parent data points(each with $|\boldsymbol{F}|$ features) to produce oversampled data point in $\boldsymbol{I}^{|\boldsymbol{F}|}$

3.2.2.2 Image Augmentation

Image augmentation is a technique commonly used in computer vision tasks, including medical image analysis, to increase the diversity of the training dataset without collecting additional data. This helps improve the performance and robustness. Image augmentation can be done by Image data generator and resize the image to 250x175.

For skin lesion images, which are often used in tasks like skin cancer classification or dermatological diagnosis, it's important to perform image augmentation carefully. Here are some techniques that are commonly used:

The original Image denoted by $I(x, y)$.

Rotation: Rotate the image by a random angle. This can help the model become invariant to rotation.
Rotation can be denoted by degrees. The mathematical notation is
Rotated Image:
$I'(x, y) = I(x.\cos(\theta) - y.\sin(\theta), x.\sin(\theta) + y.\cos(\theta))$
Flips: Flip the image horizontally or vertically. This can help the model learn invariant features.
Horizontal flip: $\boldsymbol{I'(x, y) = I(W - x, y)}$
Where W is the width of the image.
Vertical flip: $\boldsymbol{I'(x, y) = I(x, H - y)}$
Where H is the height of the image.
Zoom and Crop: Randomly zoom (by factor of α) in or out of the image and then crop it to its original size. This can help the model generalize better to different scales of lesions.
Zoomed Image: $\boldsymbol{I'(x, y) = I(\propto .x, \alpha .y)}$
Cropped Image:

$$\boldsymbol{I'(x, y) = I(x + x1, y + y1)}$$

where $x1, y1, x2, y2$ define the cropping region.

3.2.2.3 Skin lesion Segmentation

Separation of an area that was needed for analysis, or ROI, in this case, is known as segmentation of a picture. It's common for skin pictures to show both healthy and diseased parts of the skin. Attempting to process both pieces at the same time may result in a lower level of accuracy. To improve classification results, only the lesion portion should be taken into account. To isolate the lesion from the skin picture, segmentation is used.

3.2.2.3.1 Encoder and Decoder Segmentation

Figure 5 shows the CNN design for cancerous segmentation. Semantic dissection was initially suggested as a means of exploiting encoder-decoder systems. System penetration, layer arrangement, and manic aspects were all examined in the proposed system.

Four slabs, each with many convolutional, batch normalization, leaky ReLu and max-pooling layers were included in the encoder sector's initial architecture. A cross-entropy loss function-based dissection layer was used to monitor the decoder section's de-convolutional layers, batch normalization, leaky ReLu layers, and max-unpooling layers comparable to each layer in the encoder section.

The maximum-pooling covers of the encoder sector were used to create pooling catalogues that were used to up-sample the decoder section in this system. Because of the older systems' impassive totally connected layers, the encoder subdivision was smaller and the number of learnable parameters was lowered.

3.2.2.3.1.1 Encoder layers

Convolutional Layers: The encoder consists of a series of convolutional layers that extract features from the input image. Each convolutional layer applies a set of filters to the previous layer's output.
Pooling Layers: Pooling layers (e.g., max-pooling) reduce spatial dimensions and help in preserving relevant features.
Encoder Output: The final output of the encoder, denoted as *E*, represents the high-level features extracted from the input image.

3.2.2.3.1.2 Decoder

Upsampling layers: Upsampling layers increase the spatial resolution of the feature maps. Common techniques include bilinear interpolation or transposed convolutions (also known as fractionally-strided or deconvolutions).
Concatenation: In architecture, the upsampled feature maps are concatenated with corresponding feature maps from the encoder to provide context.
Convolutional Layers: The decoder also has a series of convolutional layers that process the upsampled feature maps.

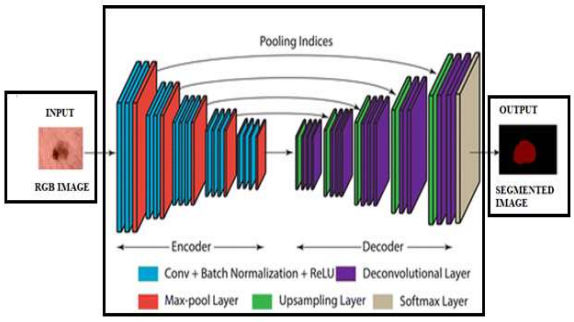

Fig5: Architecture on Encoder-Decoder Segmentation

3.2.2.3.2 Algorithm for Deep convolutional Encoder-Decoder

Encoder:
Let *I* be the input image, and **E** represents the encoder.

1. Input: Filters *Fi* and *I* denote the layer.
2. Output of the *i*-th layer can be represented as: $Oi=\sigma$ (**Fi**$*Oi-1+$**bi**)

Where σ is the activation function, **bi** is the bias term, and $*$ denotes the convolution operation.

3. The pooling operation can be represented as: Pi=pool(Oi)
4. Encoded Output represented as E = **E**(I)=Pn

Decoder:

Let D be the decoder.

1. The output of the i-th upsampling layer can be represented as: Ui=upsample($Di-1$)
2. Ci=concat(Ui,$On-i$)
3. $Di=\sigma$(**Fi′**$*Ci+$**bi′**) [process the upsampled feature maps]
4. O=**D**(E)=Dm[final output]

Loss Function:

The common loss function used in segmentation tasks is pixel-wise cross-entropy loss.

$$L(Y^{\wedge}, Y) = -N1\sum i=1N\sum j=1MYijlog(Y^{\wedge}ij) \quad (7)$$

Where $Y^{\wedge}$ is the predicted segmentation mask, Y is the ground truth mask, N is the number of pixels, and M is the number of classes.

3.2.2.4 Skin lesion Classification

3.2.2.4.1 FCN based Alex Net Framework

When compared to other transfer learning architecture, this architecture is straightforward and has a cheap computational cost. Eight weighted layers, five convolutional layers, and three fully linked layers make up the AlexNet. ReLu activation is carried out at the conclusion of each layer, with the exception of the last one, which generates a Softmax distribution over the 1000 class labels. In the first two completely linked layers, dropout is applied. Max-pooling is used after the first, second, and fifth convolutional layers, as shown in the above figure. Only those kernel mappings in the preceding layer, which are located on the same GPU, are connected to the kernels of the second, fourth, and fifth convolutional layers.

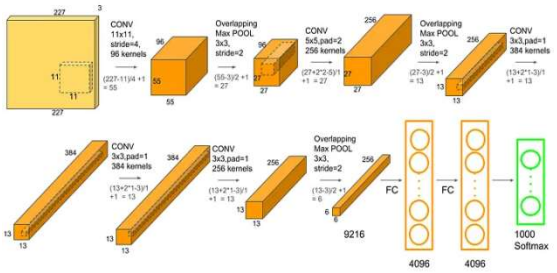

Fig.6 AlexNet architecture

3.2.2.4.2 Grouped Convolution

Grouped convolution is Alex Net's benefit. Numerous convolutions were merged into a single layer, producing multiple channels per layer. The requirement to train a network under GPU RAM constraints motivated the development of this method. The main idea was to build parallelism to lessen single-point loads. In essence, apply several kernels to the identical input images and direct them through an equivalent number of parallel training and propagation channels (more than 1). The two Alex Net paths are depicted in the model below.

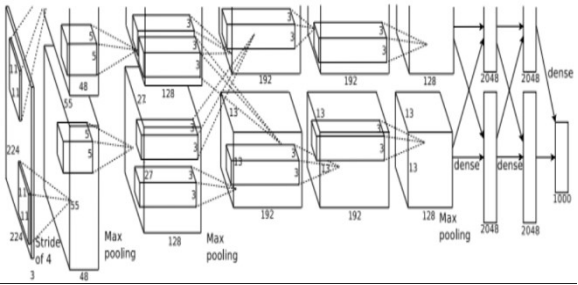

Fig.7 Two path AlexNet using Grouped Convolution

After segmenting the lesion part from the healthy part of the skin, the resultant image of the segmentation process is given as input to the FCN based AlexNet framework to do image classification with pre-trained dataset weights. Five convolutional layers, three FCN layers, and a Softmax layer make AlexNet a more robust network than other methods. Additionally, ReLu prevents vanishing gradients, dropout, data extension, and LRN address over-fitting, and several GPUs are employed to speed up computation [10]. In Fig.6, AlexNet is depicted as an FCN-based model.

Journal of Theoretical and Applied Information Technology
31st December 2023. Vol.101. No 24

ISSN: 1992-8645 www.jatit.org E-ISSN: 1817-3195

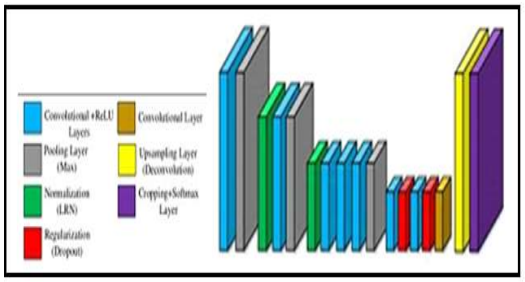

Fig.8 FCN based AlexNet Framework

In this approach, the image was resized as per AlexNet requirements. The advantage of this network is to learn the low level features and to make use of actual dataset. The AlexNet is applicable in classification and pattern recognition tasks.

Input Layer: Input to the system is resized image [3].

Convolutional Layers: In this layer, a convolution task was performed and the response sent to the next required layer. Deep convolutional layers help to learn high features or classic- specific feature [16] [6].

Max Pooling Layers: This layer is responsible for pixel representations as well as computational cost. For each feature map, max pool is applicable to find the maximum value [16].We were able to extract and reduce the size of the feature map because to the convolution and Max Pooling layers, which are fully connected. Applying completely linked layers results in the same amount of classes as before [16].This technique uses this network in the diagnosis portion because of its great performance in picture categorization.

4 RESULTS

4.1 HAM10000 Dataset

The HAM10000 dataset consist of 10015 images. The details of the image are stored in csv file with 12 parameters. The data samples are listed below.

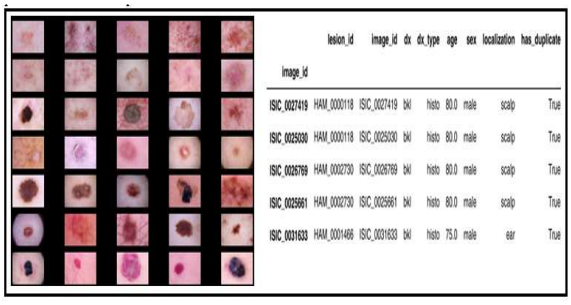

Fig.9 HAM10000 Data Samples with Skin lesion class

4.2 Exploratory Data Analysis

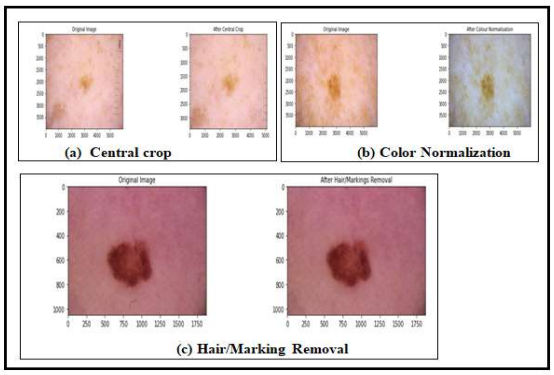

Fig.10 Exploratory Data Analysis

The stages of processed Image from original have been shown in Fig. after color normalization and hair marking removal.

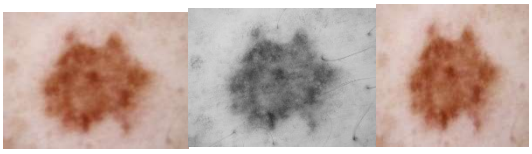

Original Image→after color normalization→ Processed Image

Fig.11 Stage of Image (original to process)

4.2.1 Image Resizing

Resize images to a uniform resolution to ensure consistency across the dataset. In Fig.9 the pre-processed image with size (380X380) has been visualized.

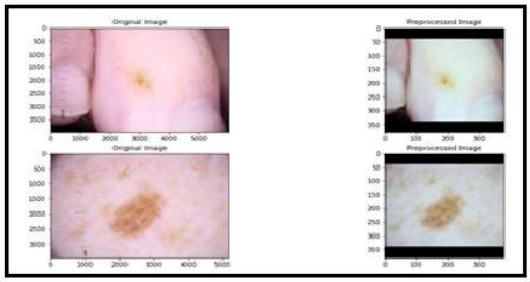

Fig.12 Pre-processed Image

4.2.2 Data and Image augmentation

To manage the data imbalance problem, augmentation has been used. In the HAM10000 dataset, the label values are not balanced. In this dataset, the lesion classes are classified as seven. The below figure shows the value count for each label in the dataset.

Journal of Theoretical and Applied Information Technology
31st December 2023. Vol.101. No 24

ISSN: 1992-8645 www.jatit.org E-ISSN: 1817-3195

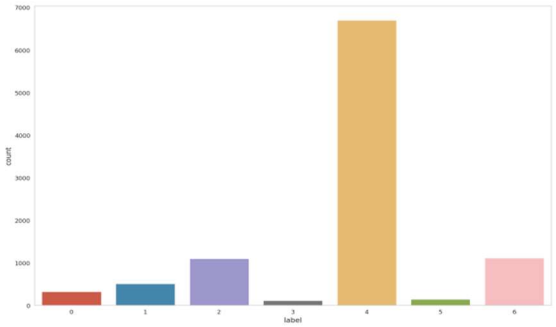

Fig.13 Lesion classes before augmentation

The skin lesion classes for the label is shown as classes = {4: ('nv', ' melanocytic nevi'),
6: ('mel', 'melanoma'),
2: ('bkl', 'benign keratosis-like lesions'),
1: ('bcc' , ' basal cell carcinoma'),
5: ('vasc', ' pyogenic granulomas and hemorrhage'),
0: ('akiec', 'Actinickeratoses and intraepithelial carcinomae'),
3: ('df', 'dermatofibroma')}

The lesion class NV labelled as 4 is extremely high when compared to others. So the dataset is completely imbalanced, and it compulsorily needs augmentation. A random sampler technique has been implemented to create a balanced dataset. The strategy value for each label has been given initially while sampling. The values for each label are given as

strategy over = {0:2000, 1:2000, 2:2000, 3:1000, 5:1000, 6:2000}

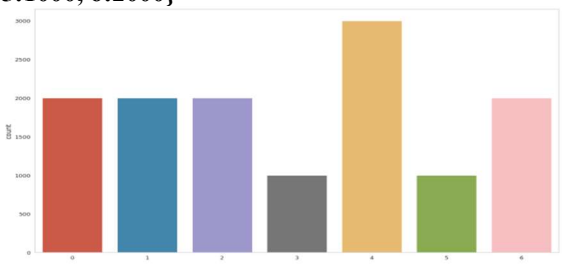

Fig.14 Lesion classes after augmentation

Image augmentation has been done by rotating the images with the angle and Flip the images in horizontal and vertical by Image data generator and it can be resized by 250X175.In Fig. the original and mask images with augmentation has been shown.

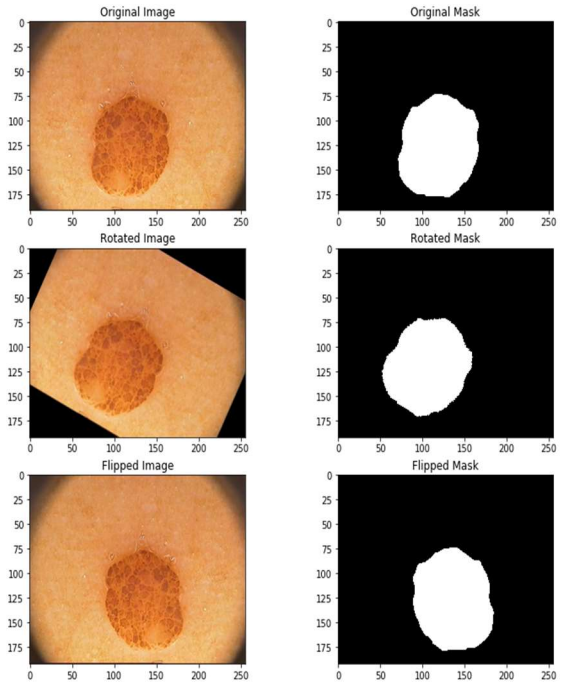

Fig.15 Image Augmentation of (Original and Mask Skin lesion)

4.2.3 Train/Test Split

The processed image has been further divided into two separate datasets train and test with a 20% and 80% split, respectively. Validation is carried out using the test data in an equal proportion. After discovering a duplicative lesion id, the dataset was partitioned.

```
Train: 0.801697453819271
Validation: 0.09915127309036445
Test: 0.09915127309036445
```

Fig.16 Data Split (Train, Test, validation)

4.3 Results on Segmentation

The results of segmentation have been visualized in Fig.17. Figure 17. (a) represents original image and respective ground truth image is in Fig.17(b).The predicted output from the original image using ground truth have been shown in Fig.17(c).The segmented output has shown in Fig.17(d).

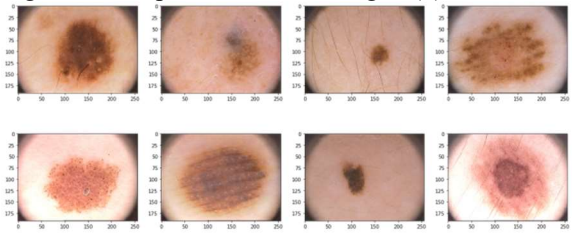

Fig.17 (a) Original Image

Journal of Theoretical and Applied Information Technology
31st December 2023. Vol.101. No 24

ISSN: 1992-8645 www.jatit.org E-ISSN: 1817-3195

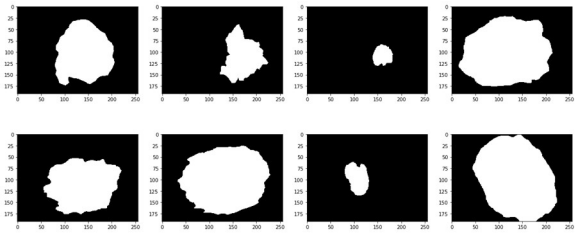

Fig.17 (b) Ground Truth Image

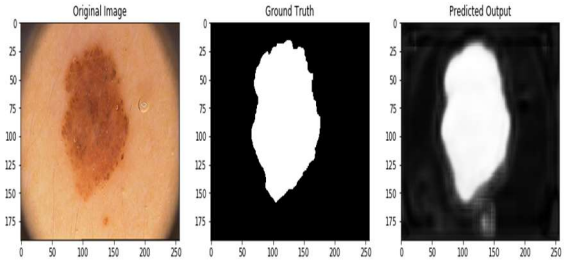

Fig.17 (c) Original Image->Ground Truth->Predicted Output

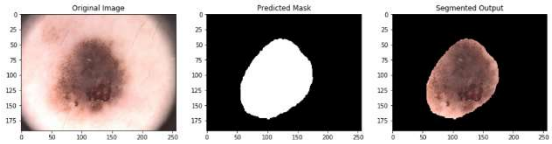

Fig.17 (d) Original Image->Predicted Mask->Segmented Output

4.3.1 Evaluation Metrics on Segmentation and Classification

4.3.1.1 Intersection over Union

A statistic for assessing the similarity and diversity of sample sets is the Jaccard index, also known as Intersection over Union and the Jaccard similarity coefficient. The size of the intersection divided by the size of the union of the sample sets defines the Jaccard coefficient, which assesses similarity between finite sample sets:

$$IoU = \frac{Intersection}{Union} \qquad (8)$$

4.3.1.2 Dice Coefficient

The Dice score is not only a measure of how many positives you find, but it also penalizes for the false positives that the method finds, similar to precision. so it is more similar to precision than accuracy.

$$Dice = \frac{2X\,TP}{(TP+FP)+(TP+FN)} \qquad (9)$$

4.3.1.3 Precision

A measure of precision counts how many correctly positive forecasts were made. Therefore, precision determines the accuracy for the minority class. It is determined by dividing the total number of correctly anticipated positive examples by the ratio of correctly predicted positive examples.

$$Precision = \frac{tp}{tp+fp} \qquad (10)$$

4.3.1.4 Recall

Recall is a metric that measures the proportion of accurate positive predictions among all possible positive predictions. Recall gives an indicator of missed positive predictions, unlike precision, which only comments on the accurate positive predictions out of all positive predictions.

$$Recall = \frac{tp}{tp+fn} \qquad (11)$$

4.3.1.5 Accuracy

An evaluation statistic called accuracy allows you to count the total number of accurate predictions made by a model. The accuracy calculation is as follows: How many of the model predictions were accurate will be determined by accuracy. True Positives and True Negatives are what accuracy considers.

$$Accuracy = \frac{No.of\ correct\ predictions}{Total\ number\ of\ input\ samples} \qquad (12)$$

4.3.1.6 Loss

Its primary method of spreading misleading information (misleading Positive) is via penalizing categorization errors. Generally speaking, multi-class classification works well. The classifier should determine a probability for each class of all the samples while using log loss.

$$Loss = -\frac{1}{N}\sum_{i=1}^{N}\sum_{j=1}^{M} y_{ij} * \log(p_{ij}) \qquad (13)$$

y_{ij} => whether sample *i* belongs to class j.
p_{ij} =>The probability of sample *i* belongs to class j.
The log loss has a range of [0,1]. A log loss that is close to zero suggests great precision, whereas one that is far from zero shows lower accuracy.
As an added bonus, minimizing log loss will increase the classifier's accuracy.

4.3.1.7 F1 Score

It falls between recall and precision harmonically. [0, 1] is its range. This statistic typically indicates how accurate (how many instances are successfully classified) and reliable (our classifier does not miss a sizable number of instances) it is.
Performance will improve the higher the F1 score. This is how it can be mathematically expressed:

Journal of Theoretical and Applied Information Technology
31st December 2023. Vol.101. No 24

ISSN: 1992-8645 www.jatit.org E-ISSN: 1817-3195

$$F1 = 2 * \frac{1}{\frac{1}{precision} + \frac{1}{recall}} \qquad (14)$$

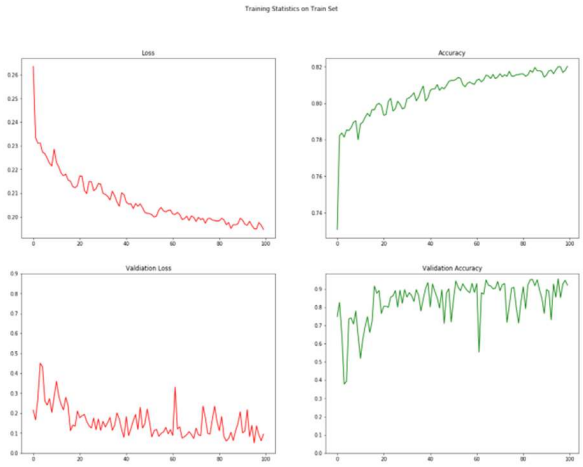

Fig.18 Training and validation statistics on Train set

Table 1: Evaluation metrics on Skin lesion segmentation using FCN based AlexNet framework

HAM10000 Dataset	IOU	Dice Coefficient	Precision	Recall	Accuracy	Loss
Training dataset	90.90	90.3	95.65	79.60	96.30	9.10
Validation	90.53	90.1	94.28	80.31	95	7.47
Testing	91.19	89.9	95.77	81.18	94.80	8.81

4.4 Results on Skin lesion classification

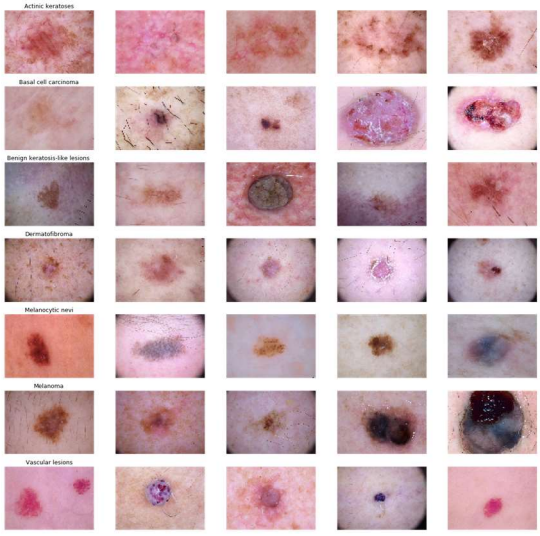

Fig. 19 (a) Skin lesion classes

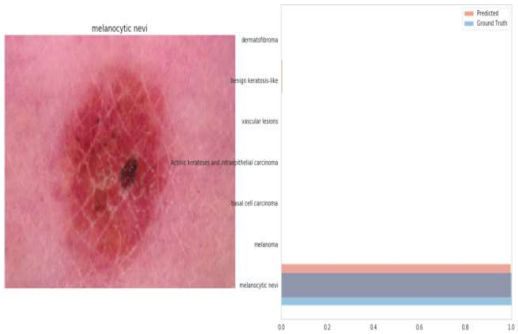

Fig.19 (b) Classification on Skin lesion class

4.4.1 Tuning Parameters on Classification

To normalize the model performance the parameters has been initialized while training. The model configures a score, a loss function, and an optimization algorithm when the layers are added. In order to evaluate the model's performance on images with known labels, a loss function is created. In other words, it's the discrepancy between actual and expected values.

The term categorical cross entropy refers to a specific categorization method. The optimizer is the most significant feature. The parameters (filter kernel value, neuron weight, and bias) of this function will be iteratively improved in order to reduce loss.

Since the stochastic gradient descent has two extensions, the Adam optimizer was chosen since it incorporates the advantages of both of them. Per-parameter learning is maintained using the Adaptive Gradient Algorithm (AdaGrad).

RMSProp keeps a learning rate for each parameter that is updated based on the average of recent gradient magnitudes for the weight.

Adam favors in-depth training above surface knowledge because of his need for immediate gratification. The "precision" measure is used to evaluate our model's performance. Because it doesn't employ metric evaluation results to train the model like the loss function (for evaluation only).

It is faster and closer to the loss function's overall minimum when the annealing approach with a learning rate is utilized (LR). The loss context is traversed by the optimizer in LR. Reduce the rate at which you learn in order to minimize your losses. Rapid computation times with high LR can be maintained by dynamically decreasing the LR as needed every X steps (epochs) (when accuracy is not improved).

The accuracy and loss of the training and validation has been shown in Fig.20 and the score visualized in Table.2.

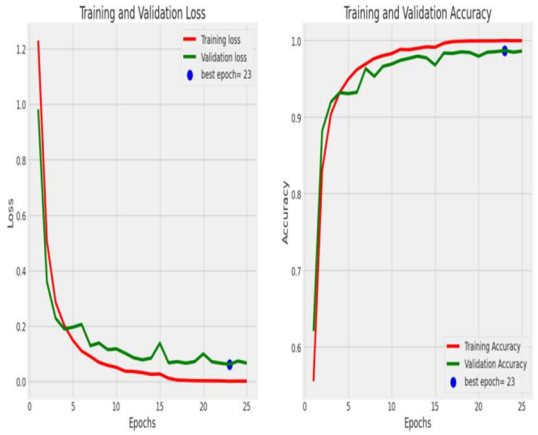

Fig.20 Accuracy and loss of skin lesion classification

Table.2: Evaluation metrics on Skin lesion classification using FCN based AlexNet framework

HAM10000 Dataset	Accuracy	Loss
Training dataset	99.99	0.00039
Validation	98.69	0.0615
Testing	98.61	0.0661

4.4.2 Evaluation Metric on Classification

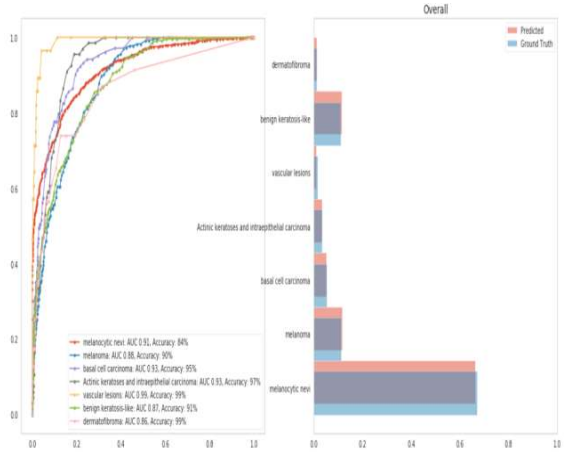

Fig. 21 AUC and Accuracy of Skin lesion class with Predicted and Ground Truth

Table.3: Classification report of skin lesion class

Skin lesion class	Precision	Recall	F1-Score	AUC	Accuracy
Melanocytic Nevi	0.88	0.82	0.88	0.91	84%
Melanoma	0.86	0.92	0.90	0.88	90%
Basal cell carcinoma	0.96	0.94	0.95	0.93	95%
Actinic Keratoses and Intraepthellal carcinoma	0.97	0.98	0.97	0.93	97%
Vascular lesions	0.99	1.00	0.99	0.99	99%
Benign keratosis	0.96	0.89	0.91	0.87	91%
Dermatofibroma	0.99	1.00	0.99	0.86	99%

5 DISCUSSION

The results are compared with state of art methods. For skin lesion segmentation the model performance on FCN AlexNet framework. The table shows the comparison of the various model performances.

Table.4: Comparison on various state of art methods for skin lesion segmentation

Model	Dataset	Accuracy (%)	Dice
EIU-net (Yu, Z et.al 2023)[17]	ISIC 2016	-	0.919
	ISIC 2017		0.855
	ISIC 2018		0.902
	PH2		0.916
E-GAN(Innani,et.al 2023)[18]	ISIC 2018	94.5	0.901
FCN-Res AlexNet (Barın,et.al,2022) [19]	ISIC 2017	93.47	0.8735
FCN -8s (Kaymak ,et.al,2020)[20] FCN -16s FCN -32s	ISIC2018	93.9 93.7 93.7	0.841 0.833 0.826
Proposed FCN based AlexNet	**ISIC2018**	**95**	**0.901**

Table.5: Comparison on state of art methods with proposed work for skin lesion classification

Model	Dataset	Accuracy
Augmentation with AlexNet(Hosny K et.al,2019)[21]	ISIC2017	95.91%
Modified (MobileNetV2+VGG16+C-SVM) (Bibi, A et.al,2022)[22]	HAM10000	96.7%

Double Branch Network (Wang, H et.al,2023)[23]		91.58%
EfficientNetB0 (Koppolu, B. P. (2023).[24]		93.50%
CNN with 3 layers(Nancy.V et.al,2023)[25]		98.02%
MobileNetv2(Nancy.V et.al,2023)[25]		97.58%
Proposed Model(FCN based AlexNet Framework)		**98.69%**

6 CONCLUSION AND FUTURE WORK

This proposed method being effective to eliminate the subjectivity in visual interpretation of dermoscopy pictures and decrease the amount of false- negative/false-positive diagnoses by introducing a new method for measuring abrupt cut-off and increasing the performance of segmentation and classification algorithms. While reviewing algorithms for predictions on skin cancer deep learning models works on image dataset well and the accuracy achieved was high when compare to machine learning algorithms. The proposed method concluded that FCN based AlexNet model is suitable for prediction on melanoma tumor in efficient way by two process namely Skin lesion segmentation using Encoder and Decoder Segmentation with accuracy of 95% and dice coefficient with 0.901, Classification with accuracy as 98.61%. In future, to improve accuracy, transfer learning model with CNN can be done. In order to prevent the problem of over fitting and to ensure that the dataset is balanced, the augmentation process also included an increase in the dataset to properly train the model.

REFERENCES:

[1] Adegun, A. A., & Viriri, S. (2020). FCN-based DenseNet framework for automated detection and classification of skin lesions in dermoscopy images. *IEEE Access*, *8*, 150377–150396. https://doi.org/10.1109/access.2020.3016651

[2] Albahar, M. A. (2019). Skin lesion classification using convolutional neural network with novel regularizer. *IEEE Access*, *7*, 38306–38313. https://doi.org/10.1109/access.2019.2906241

[3] Ashraf, R., Afzal, S., Rehman, A. U., Gul, S., Baber, J., Bakhtyar, M., Mehmood, I., Song, O.-Y., & Maqsood, M. (2020). Region-of-interest based transfer learning assisted framework for Skin cancer detection. *IEEE Access*, *8*, 147858–147871. https://doi.org/10.1109/access.2020.3014701

[4] Farooq, M. A., Azhar, M. A., & Raza, R. H. (2016). Automatic lesion detection system (ALDS) for skin cancer classification using SVM and Neural Classifiers. *2016 IEEE 16th International Conference on Bioinformatics and Bioengineering (BIBE)*. https://doi.org/10.1109/bibe.2016.53

[5] Hosny, K. M., Kassem, M. A., & Foaud, M. M. (2018). Skin cancer classification using Deep Learning and Transfer Learning. *2018 9th Cairo International Biomedical Engineering Conference (CIBEC)*. https://doi.org/10.1109/cibec.2018.8641762

[6] Hosny, K. M., Kassem, M. A., & Fouad, M. M. (2020). Classification of skin lesions into seven classes using transfer learning with AlexNet. *Journal of Digital Imaging*, *33*(5), 1325–1334. https://doi.org/10.1007/s10278-020-00371-9

[7] Lakhtakia, R., Mehta, A., & Nema, S. K. (2009). Melanoma : A frequently missed diagnosis. *Medical Journal Armed Forces India*, *65*(3), 292–294. https://doi.org/10.1016/s0377-1237(09)80036-1

[8] M, V. M. (2019). Melanoma skin cancer detection using image processing and machine learning. *International Journal of Trend in Scientific Research and Development*, *Volume-3*(Issue-4), 780–784. https://doi.org/10.31142/ijtsrd23936

[9] Mane, S., & Shinde, S. (2018). A method for melanoma skin cancer detection using dermoscopy images. *2018 Fourth International Conference on Computing Communication Control and Automation (ICCUBEA)*. https://doi.org/10.1109/iccubea.2018.8697804

[10] Marks, R. (1995). An overview of skin cancers. *Cancer*, *75*(S2), 607–612. https://doi.org/10.1002/1097-0142(19950115)

[11] Melanoma skin cancer classification using deep learning Convolutional Neural Network. (2020). *Medico-Legal Update*. https://doi.org/10.37506/mlu.v20i3.1421

[12] Mind, D. S.- D. (n.d.). *Umělá inteligence, machine learning a neuronové sítě*. Data Science - Data Mind. Retrieved December 16, 2021, from http://www.datamind.cz/cz/Sluzby-Data-Science/umela-intelingence-AI-ML-machine-learning-neural-net

[13] Mukherjee, S., Adhikari, A., & Roy, M. (2019). Malignant melanoma classification using cross-platform dataset with deep learning

CNN Architecture. *Recent Trends in Signal and Image Processing*, 31–41. https://doi.org/10.1007/978-981-13-6783-0_4

[14] Munia, T. T., Alam, M. N., Neubert, J., & Fazel-Rezai, R. (2017). Automatic diagnosis of melanoma using linear and nonlinear features from Digital Image. *2017 39th Annual International Conference of the IEEE Engineering in Medicine and Biology Society (EMBC)*. https://doi.org/10.1109/embc.2017.8037802

[15] R D, S., & A, S. (2019). Deep learning based skin lesion segmentation and classification of melanoma using support Vector Machine (SVM). *Asian Pacific Journal of Cancer Prevention*, *20*(5), 1555–1561. https://doi.org/10.31557/apjcp.2019.20.5.1555

[16] Romero-Lopez, A., Giro-i-Nieto, X., Burdick, J., & Marques, O. (2017). Skin lesion classification from dermoscopic images using Deep Learning Techniques. *Biomedical Engineering*. https://doi.org/10.2316/p.2017.852-053

[17] Yu, Z., Yu, L., Zheng, W., & Wang, S. (2023b). EIU-net: Enhanced feature extraction and improved skip connections in U-Net for skin lesion segmentation. *Computers in Biology and Medicine*, *162*, 107081. https://doi.org/10.1016/j.compbiomed.2023.107081

[18] Innani, S., Dutande, P., Baid, U., Pokuri, V., Bakas, S., Talbar, S., Baheti, B., & Guntuku, S. C. (2023a). Generative adversarial networks based skin lesion segmentation. *Scientific Reports*, *13*(1). https://doi.org/10.1038/s41598-023-39648-8

[19] Barın, S., & Güraksın, G. E. (2022). An automatic skin lesion segmentation system with hybrid FCN-resalexnet. *Engineering Science and Technology, an International Journal*, *34*, 101174. https://doi.org/10.1016/j.jestch.2022.101174

[20] Kaymak, R., Kaymak, C., & Ucar, A. (2020). Skin lesion segmentation using fully convolutional networks: A Comparative Experimental Study. *Expert Systems with Applications*, *161*, 113742. https://doi.org/10.1016/j.eswa.2020.113742

[21] Hosny, K. M., Kassem, M. A., & Foaud, M. M. (2019). Classification of skin lesions using transfer learning and augmentation with Alex-Net. *PLOS ONE*, *14*(5). https://doi.org/10.1371/journal.pone.0217293

[22] Bibi, A., Attique Khan, M., Younus Javed, M., Tariq, U., Kang, B.-G., Nam, Y., R. Mostafa, R., & H. Sakr, R. (2022). Skin lesion segmentation and classification using conventional and deep learning based framework. *Computers, Materials & Continua*, *71*(2), 2477–2495. https://doi.org/10.32604/cmc.2022.018917

[23] Wang, H., Qi, Q., Sun, W., Li, X., & Yao, C. (2023). Classification of clinical skin lesions with double-branch networks. *Frontiers in Medicine*, *10*. https://doi.org/10.3389/fmed.2023.1114362

[24] Koppolu, B. P. (2023). Skin lesion classification using transfer learning. *2023 International Conference on Intelligent Data Communication Technologies and Internet of Things (IDCIoT)*. https://doi.org/10.1109/idciot56793.2023.10053478

[25] Nancy, V. A., Prabhavathy, P., Arya, M. S., & Ahamed, B. S. (2023). Comparative study and analysis on skin cancer detection using machine learning and deep learning algorithms. *Multimedia Tools and Applications*. https://doi.org/10.1007/s11042-023-16422-6

[26] Sumithra, R., Suhil, M., & Guru, D. S. (2015). Segmentation and classification of skin lesions for disease diagnosis. *Procedia Computer Science*, *45*, 76–85. https://doi.org/10.1016/j.procs.2015.03.090

[27] Lynn, N. C., & Kyu, Z. M. (2017). Segmentation and classification of skin cancer melanoma from skin lesion images. *2017 18th International Conference on Parallel and Distributed Computing, Applications and Technologies (PDCAT)*. https://doi.org/10.1109/pdcat.2017.00028

[28] Ünver, H. M., & Ayan, E. (2019). Skin lesion segmentation in dermoscopic images with combination of Yolo and GrabCut algorithm. *Diagnostics*, *9*(3), 72. https://doi.org/10.3390/diagnostics9030072